High order and conservative method for patched grid interfaces

B. Maugars, B. Michel, P. Cinnella

High order and conservative method for patched grid interfaces

B. Maugars* and B. Michel †

ONERA - The French Aerospace Lab, F-92322 Châtillon, France

P. Cinnella ‡

Laboratoire DynFluid, Arts et Metiers ParisTech, 151 bvd de l´Hôpital, 75013 Paris, France

A high-order and conservative method is developed for the numerical treatment of interface conditions in patched grids, based on the use of a fictitious grid methodology. The proposed approach is compared with a non-conservative interpolation of the state variables from the neighbouring domain for selected internal flow problems.

I. Introduction

Turbomachinery configurations are dominated by the relative motion of fixed and mobile wheels. The resulting flow field is highly unsteady, and the understanding and control of rotor/stator interactions is of paramount importance for aerodynamic, aeroelastic and aeroacoustic design. For this purpose, advanced simulation tools like Large Eddy Simulation (LES) and Detached Eddy Simulation (DES) are being applied to turbomachinery configurations in order to improve the description of the unsteady flow field. For this type of advanced modeling, the use of high-order numerical schemes is mandatory, to ensure low levels of numerical errors despite the relatively coarse and distorted grids typically available for industrial configurations (see, e.g.[1]). To achieve a truly high-order overall accuracy, boundary conditions need to be also high order. Inter-wheel interfaces typically involve patched grids due to geometrical constraints and to the relative motion between adjacent wheels (see Figure 1). Patched grid interface conditions were described for the first time in the work of Rai.[2,3] Thomas[4] proposed another method for non-conformal meshes and applied it to an industrial case. Later, Lerat and Wu[5] developed an implicit boundary treatment and studied stability. All these methods are conservative low-order (first and second order accuracy at most). Tucker[6,7] discusses requirements for high-quality turbomachinery simulations with focus on boundary conditions. Turbomachinery calculations using high order finite difference(FD) with non-conformal mesh have recently been carried out by Rai:[8,9] inter-stage coupling is made through fourth-order accurate interpolations, but the method is not conservative. A conservative approach is necessary to avoid mass flow and momentum losses. In addition, the work of Part-Enander[10] and Berger[11,12] shows that the lack of conservation also affects the prediction of shocks, more particularly slow unsteady shocks. Moreover, Wu[13] develops several conservative and non-conservative overlapping mesh methods and notes that conservative methods allow the passage of unsteady shocks without delay across interfaces.

In this work we develop a high-accurate conservative method for patched grid interfaces. To set-up and assess the accuracy and conservation of the proposed method, we initially consider a simplified framework, namely, patched two-dimensional Cartesian grids. Afterwards, the methodology is extended to non Cartesian patched grids. Preliminary applications to a transonic turbine cascade are also shown.

The paper is organized as follows: Section II briefly recalls the governing equations and describes the numerical schemes applied at inner-points. Section III presents two interface treatments for structured grids: a high-order non conservative method based on variable interpolation in ghost cells, and a high-order and

*Phd student, ONERA, Computational Fluid Dynamics and Aeroacoustics Department, AIAA Member

†Research engineer, ONERA, Computational Fluid Dynamics and Aeroacoustics Department, AIAA Member

‡Professor, Laboratoire DynFluid, Paris, Senior AIAA member.

conservative method based on the use of a fictitious grid. In the last case, it is shown that, to achieve an overall order greater than two, some consistent Finite Volume (FV) approximation has to be used both for the interface and the inner-point discretization scheme. Finally, results are shown for problems of increasing complexity, including turbomachinery applications.

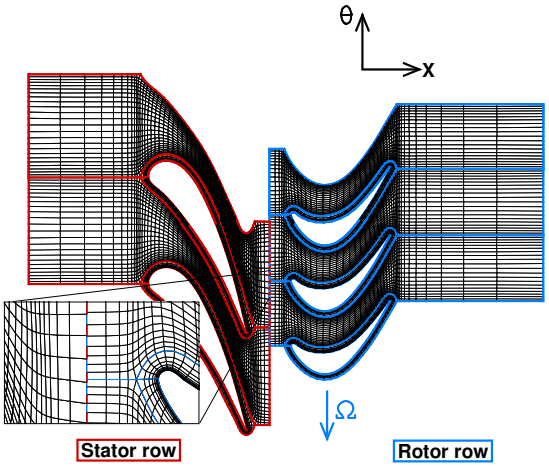

Figure 1. Example of rotor/Stator configuration and blow-up of the patched grid at rotor/stator interface.

II. Governing Equations and Numericals Schemes

In this paper, we restrict our attention to steady inviscid flows. For simplicity, numerical schemes are described for the following 2D hyperbolic problem:

$$w_t + f_x + g_y = 0 \tag{1}$$

We consider a computational domain discretized using Cartesian grid of steps δx and δy space in x and y directions respectively. Grid points are identified by the indices (i, j). Since the treatment of patched grid interfaces affects the spatial accuracy of the numerical method, hereafter we focus on semi-discrete schemes in space. For this purpose, we introduce the difference and average operators, denoted by δ and μ, respectively, in each space direction (denoted 1 and 2):

$$\begin{aligned}(\delta_1 f)_{i+\frac{1}{2},j} &= f_{i+1,j} - f_{i,j} \ ; \ (\mu_1 f)_{i+\frac{1}{2},j} = \frac{1}{2}(f_{i+1,j} + f_{i,j}) \\ (\delta_2 f)_{i,j+\frac{1}{2}} &= f_{i,j+1} - f_{i,j} \ ; \ (\mu_2 f)_{i,j+\frac{1}{2}} = \frac{1}{2}(f_{i,j+1} + f_{i,j})\end{aligned} \tag{2}$$

To discretize Equation (1), we consider two different formulations: the finite difference (FD) formulation is obtained by replacing space derivatives in (1) by differences approximations. We then obtain the semi-discrete equation in space:

$$w_t + r(w) = 0 \tag{3}$$

with $r(w)$ a spatial discretization operator. In a FD framework, a scheme is accurate at order q if its truncation error is such that:

$$\epsilon = u_t + r(u) = O(h^q) \tag{4}$$

where u is an exact solution of (1) and $h = max(\delta x, \delta y)$ a characteristic mesh size. Moreover, the FD scheme is said to be conservative if it is possible to write the operator r under the form:

$$r(w) = \frac{(\delta_1 F)_{i,j}}{\delta x} + \frac{(\delta_2 G)_{i,j}}{\delta y} \tag{5}$$

where F and G are the numerical fluxes in the directions 1 and 2 of the mesh, defined respectively at $(i+\frac{1}{2}, j)$ and $(i, j+\frac{1}{2})$.
In this work we consider a family of high-order schemes constructed through recursive truncation error correction of the standard second-order centred scheme[14] . A built-in numerical dissipation term is obtained by upwinding the correction (See Ref.[15]), so that schemes belonging to this family are odd-order accurate, i.e. order $2p+1$ with p an integer and make use of a stencil of $2p+3$ points in each direction. Their numerical flux in the x direction writes :

$$F^{FD(2p+1)}_{i+\frac{1}{2},j} = \left(I + a_1\delta_1^2 + \cdots + a_p\delta_1^{2p}\right)\mu_1 f_{i+\frac{1}{2},j} - \left(\frac{a_p}{2}|A_R|\delta^{2p+1}w\right)_{i+\frac{1}{2},j} \tag{6}$$

where A_R is the Roe average, and $a_1, \ldots, a_p$ are coefficients selected in such a way as to nullify error terms up to order $2p$. Similar expressions hold for the numerical flux $G_{i,j+\frac{1}{2}}$ in the second mesh direction. To fix ideas, we provide hereafter the numerical fluxes of $FE - MUSCL$ schemes of order 3 and 5:

$$\begin{aligned} F^{FD3}_{i+\frac{1}{2},j} &= \left(I - \frac{1}{6}\delta_1^2\right)\mu_1 f_{i+\frac{1}{2},j} - \left(\frac{1}{12}|A_R|\delta_1^3 w\right)_{i+\frac{1}{2},j} \\ F^{FD5}_{i+\frac{1}{2},j} &= \left(I - \frac{1}{6}\delta_1^2 + \frac{1}{30}\delta_1^4\right)\mu_1 f_{i+\frac{1}{2},j} + \left(\frac{1}{60}|A_R|\delta_1^3 w\right)_{i+\frac{1}{2},j} \end{aligned} \tag{7}$$

The finite volume formulation (FV) is obtained from the integral form of the governing equations:

$$\frac{d}{dt}\int_{\Omega_{i,j}} w d\Omega + \oint_{\partial\Omega_{i,j}} \mathbf{f}\cdot\mathbf{n} d\Gamma = 0 \tag{8}$$

where $\mathbf{f} = (f, g)$, and $\Omega_{i,j}$ is a control volume with border $\partial\Omega_{i,j}$ and outer unit normal $\mathbf{n}$. The FV discretization requires to define approximations of volume and surface integrals in Equation (8). Hereafter we focus on cell-centered FV schemes, for which the unknowns are either the mean values of w over a mesh cell, or the pointwise values of w at cell centroids.

A FV scheme is q^{th}-order accurate if the volume and surface integrals are approximated at order q.[16] A semi-discrete FV scheme may be written as:

$$|\Omega_{i,j}|(\mathcal{I}w_t)_{i,j} + \sum_{\Gamma\in\partial\Omega_{i,j}} |\Gamma| F_\Gamma(w_{p,p\in D_\Gamma}, \mathbf{n_\Gamma}) = 0 \tag{9}$$

where F_Γ denotes the numerical flux through face Γ of measure $|\Gamma|$, which depends on the values of w at points p in the domain of dependance D_Γ. The first term represents a discretization of the volume integral in Eq. (8), whereas the numerical flux represents a discretization of the mean flux density $\frac{1}{|\Gamma|}\int_\Gamma \mathbf{f}\cdot\mathbf{n} d\Gamma$ on face Γ. The semi-discrete scheme is said to be conservative if:

$$F_\Gamma(w_{p,p\in D_\Gamma}, \mathbf{n_\Gamma}) = -F_\Gamma(w_{p,p\in D_\Gamma}, -\mathbf{n_\Gamma}) \tag{10}$$

In Ref,[14] it is shown that, for 1D problems, the high-order numerical fluxes (7) can be equivalently derived in a FV framework by means of MUSCL flux extrapolation formulae. This is why schemes (7) are referred-to as FE-MUSCL in the following. For 2D problems, application of 1D numerical fluxes to each mesh direction separately does not ensure high-order accuracy on general curvilinear grids. For this reason we consider hereafter several strategies for constructing high-accurate multidimensional FV approximations.

The first one is a straightforward extension of finite-difference schemes to a FV framework: the identity operator ($\mathcal{I} = Id$) is used for the approximation of the first term in Equation 8 and the numerical fluxes of

the FD scheme are used to approximate surface integrals. This approach is first order accurate at most in the FV sense (see e.g.[16]), but allows recovering high-order accuracy in the FD sense on regular Cartesian grids, since the resulting discretization is equivalent to the FD scheme applied to the grid made by cell centers.

A truly high-order FV extension to general curvilinear meshes of the third-order FE-MUSCL scheme was developed by Rezgui et al.[16] by using weighted discretization operators to take into account mesh deformations. On the other hand, Saunier et al.[17] developed a FV extension on on Cartesian grids of the fifth-order scheme.

Both of these extensions are constructed by taking the state variables at cell centers (i,j) as the problem unknowns. On regular Cartesian grids, numerical fluxes of the schemes of order 3 and 5 write, respectively:

$$\begin{aligned} F^{FV3}_{i+\frac{1}{2},j} &= \underbrace{\left(I-\frac{1}{8}\delta_1^2\right)\mu_1 f_{i+\frac{1}{2},j}}_{flux\ density} + \underbrace{\left(\frac{1}{24}\delta_2^2\right)\mu_1 f_{i+\frac{1}{2},j}}_{Integration} - \underbrace{\left(\frac{1}{12}|A_R|\delta_1^3 w\right)_{i+\frac{1}{2},j}}_{Dissipation} \\ F^{FV5}_{i+\frac{1}{2},j} &= \underbrace{\left(I-\frac{1}{8}\delta_1^2+\frac{3}{128}\delta_1^4\mu_1\right)f_{i+\frac{1}{2},j}}_{flux\ density} + \underbrace{\left(\frac{1}{24}\delta_2^2-\frac{51}{17280}\delta_2^4-\frac{1}{192}\delta_1^2\delta_2^2\right)\mu_1 f_{i+\frac{1}{2},j}}_{Integration} + \underbrace{\left(\frac{1}{60}|A_R|\delta_1^3 w\right)_{i+\frac{1}{2},j}}_{Dissipation} \end{aligned} \tag{11}$$

The preceding expressions are composed by three terms: the first one is a high order approximation of the flux density at the center of a cell face, the second one comes from the integration of the flux density along the interface, and the last one is a numerical dissipation term. In the following, these schemes are directly applied to curvilinear grids by using the same coefficients corresponding to Cartesian grids. As a consequence, the nominal order of accuracy is not necessarily preserved on general grids.

For further convenience, we also introduce FV numerical fluxes obtained from Equations (11) by removing the face integration term (noted $FV-WI$, for "without integration"):

$$\begin{aligned} F^{FV3-WI}_{i+\frac{1}{2},j} &= \left(I-\frac{1}{8}\delta_1^2\right)\mu_1 f_{i+\frac{1}{2},j} - \left(\frac{1}{12}|A_R|\delta_1^3 w\right)_{i+\frac{1}{2},j} \\ F^{FV3-WI}_{i+\frac{1}{2},j} &= \left(I-\frac{1}{8}\delta_1^2+\frac{3}{128}\delta_1^4\right)\mu_1 f_{i+\frac{1}{2},j} + \left(\frac{1}{60}|A_R|\delta_1^3 w\right)_{i+\frac{1}{2},j} \end{aligned} \tag{12}$$

The last and more general (and computationally expensive) FV strategy used in this work is a Godunov-type method based again on Roe's approximate Riemann solver, which uses k-exact reconstructions (initially introduced in Ref.[18]) of the solution over a cell from the cell-averaged values of the state variables to calculate the left and right states at cell interface and to compute volume and surface integrals. Precisely, we consider here a k-exact scheme based on an efficient successive reconstruction of the solution and its derivatives, up to the desired order of accuracy[19] . Thanks to high-order reconstructions, this approach ensures truly high-order accuracy on general curvilinar grids. Schemes of this family are referred-to in the following as k-exact schemes, with k an integer correponding to the order of the reconstruction in use.

III. Patched-grid Interfaces

In the remainder of this study, we consider for simplicity the 2D Cartesian setting illustrated in Figure 2. Each block is equipped with several layers of ghost cells, according to the stencil of the inner scheme used, which allows processing each block independently. Ghost cells of each block are overlapped by the physical cells of the neighboring block. Hereafter, we consider and compare two different techniques to exchange information through the interface.

III.A. Overlapping Grid Method

This method consist in interpolating at the desired order the conservative variables in the ghost cells of a block from the overlapping inner cells of the adjacent block, so that each block can be treated independently.

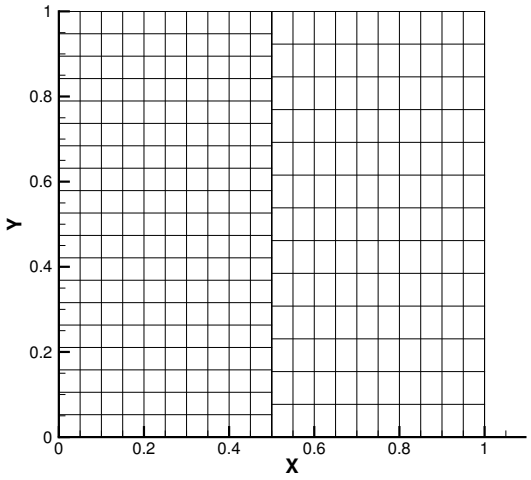

Figure 2. Cartesian patched grid

The drawback of this methodology is that it does not ensure conservation since, for nonlinear problems, numerical fluxes on each side of the patched interface are generally not the same.

Figure 3 provides a sketch of the interpolation method for an interpolation stencil leading to second-order

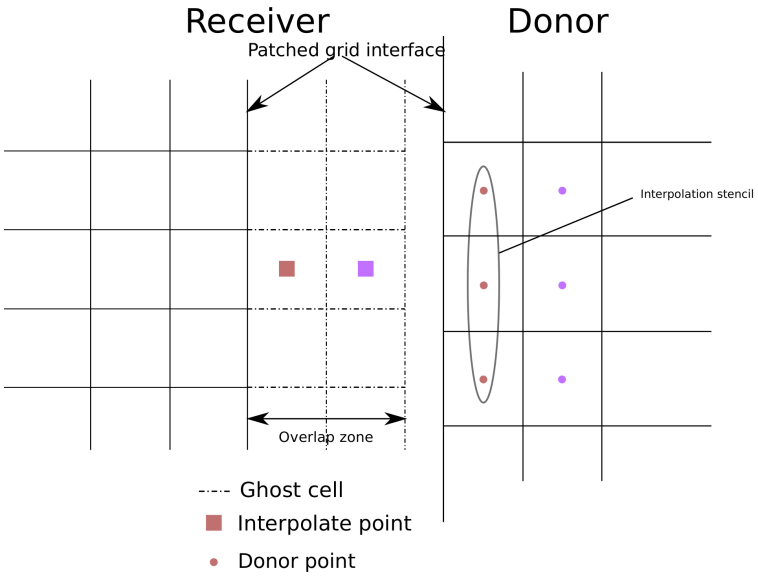

Figure 3. Overlapping grid interpolation scheme.

accuracy. Extension to 3D problems is straightforward. This method is high order in the sense of truncation error: if interpolations are made at the same order of numerical scheme used to discretize the inner cells, theoverall convergence of the solution is of the same order.

III.B. Fictitious Grid Method

In the quest for a high-order and conservative method, we investigate hereafter a methodology based on the use of a fictitious grid encompassing the interface. This can be seen as a high-order extension of the one

proposed in Ref. 5. The fictitious grid is constructed by prolongation and intersection of inner grids from the two adjacent blocks on either side of the interface, as shown in Figure 4. The number of cells of the fictitious grid in the direction normal to the interface is selected according to the discretization stencil of the inner scheme. For instance, in Figure 4, the number of ghost cells is suitable for numerical schemes using a stencil with five mesh points per direction at most.

At the present stage, the procedure is restricted to interfaces such that surface vectors on both sides are collinear. It will be generalized to curved interfaces in further work. Once the fictitious grid has been constructed, state vectors from the physical grids on each side of the interface are interpolated to the fictitious grid cell centers by means of high-order Lagrange polynomials. Then, information from the fictitious cell-centers is used to construct a high-order approximation of the flux densities at centers of interface cell faces. For this purpose, we use formulae given in Equation (12), which correspond to a high-order reconstruction of the physical flux at a face center from the surrounding cell-center values.

Finally, the reconstructed flux densities are integrated along the face by means of a high-order quadrature formula to get the integrated numerical fluxes at the interface. The final step consists in distributing fluxes to both sides of the interface in a conservative way. Precisely, denoting with the superscripts 1 and 2 interface numerical fluxes assigned to blocks 1 and 2 on each side of the interface, and with superscript g numerical fluxes computed on the ficticious grid, conservation is guaranted if these satisfy the distribution rule of Equation 13.

$$\begin{cases} F^1_{i+\frac{1}{2},j}\mathbf{\Gamma_{i+\frac{1}{2},j}} = F^g_{n+\frac{1}{2},p}\mathbf{\Gamma_{n+\frac{1}{2},p}} + F^g_{n+\frac{1}{2},p+1}\mathbf{\Gamma_{n+\frac{1}{2},p+1}} \\ F^2_{l-\frac{1}{2},m}\mathbf{\Gamma_{l-\frac{1}{2},m}} = -F^g_{n+\frac{1}{2},p-1}\mathbf{\Gamma_{n+\frac{1}{2},p-1}} - F^g_{n+\frac{1}{2},p}\mathbf{\Gamma_{n+\frac{1}{2},p}} \end{cases} \tag{13}$$

where $\mathbf{\Gamma}$ denotes an oriented surface.

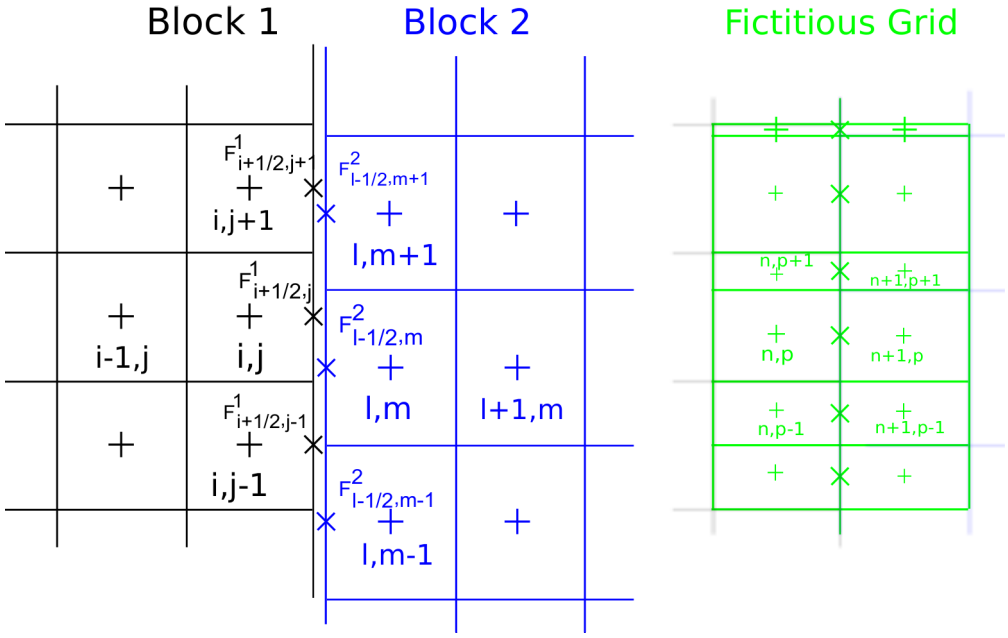

Figure 4. Fictitious grid construction and notations.

Hereafter, we briefly discuss the impact of the fictitious grid interface treatment on the overall solution accuracy. This strongly depends on interactions between the interface treatment and the inner-point discretization scheme. We already pointed out in Section II that, if the inner point discretization scheme is based on a straightforward extension of FD fluxes to curvilinear grids via a FV formulation, overall high-order accuracy in the FD sense (high-order approximation of space derivatives) is achieved on a Cartesian grid, since the approximation degenerates to a high-order FD scheme applied to the dual grid. If however, a patched grid is used, than numerical fluxes along the patched interface are approximated in a different way with respect to inner point fluxes. The reason is that a high-order integration of the fluxes along the interface is required to ensure the conservation condition, whereas a simple second-order integration formula

along faces is used for inner cells. By carrying out Taylor series expansions, it is possible to prove that this introduces a 2nd-order error term that vanishes only if points on each side of the interface are coincident, i.e. for a perfect match condition. Due to this error, the overall accuracy cannot be higher than two even if the inner point scheme applied to each cell block is nominally higher-order accurate, and the grids on both sides of the patched interface are Cartesian.

Similarly, it is possible to prove that, if an accurate FV formulation is used to discretize inner cells and, specifically, high-order integration of the fluxes along cell faces is carried out, then the inner point fluxes are consistent with the interface fluxes, and errors cancel up to the order of accuracy of the approximation used to compute surface integrals.

III.C. Summary

In this section, two kind of patched interface tratments have been developed: the first one, based on high-order Lagrange interpolations of state variables in ghost cells associated to neighbouring blocks, ensure overall high-order accuracy of the solution but does not ensure conservation. As an alternative, we considered a fictitious grid method, which reconstructs high order fluxes on a fictitious grid given by the intersection of the neighboring grids augmented by their ghost cells. The resulting fluxes are then integrated along the interface and distributed to neighboring grids. Even if this proceduce allows reconstructing fluxes along the interface at high-order, achieving overall high-order accuracy of the numerical solution requires using a formulation of the inner-point numerical fluxes that is consistent to that used on the interface. The consequence is that, if straightforward extensions of FD numerical fluxes are applied at inner interfaces, the overall accuracy sticks to order two at most, whereas higher accuracy can be achieved by using accurate FV approximations for the inner point scheme. In the following we provide numerical proofs of this statement for selected test cases.

IV. Results

The preceding patched interface treatments are applied hereafter to selected test cases, and their ability to ensure high-order accuracy and conservation is assessed.

IV.A. Circular Advection of a Gaussian Pulse

The first test case is the circular advection of a Gaussian function in domain $[0,1]\times[0,1]$n around the point $(x=1,y=0)$. We therefore seek a steady solution of the following problem:

$$\begin{cases} \dfrac{\partial w}{\partial t} + y\dfrac{\partial w}{\partial x} + (1-x)\dfrac{\partial w}{\partial y} = 0, 0<x<1, 0<y<1 \\ w(x,y,0) = 0, 0<x<1, 0<y<1 \\ w(x,0,t) = \exp(-50.0\cdot(x-0.5)^2) \end{cases} \tag{14}$$

The exact steady solution, shown in Figure 5, is $w = w(x,0,t)$ on any circle with center (1,0). The computational domain is discretized by patched grids composed by two domains: $[0,0.5]\times[0,1]$ and $[0.5,1]\times[0,1]$. Both domains are discretized by regular Cartesian grids, connected by a patched interface. A series of grids of increasing density is constructed to investigate the overall convergence of the numerical solution as a function of a characteristic mesh size. Numerical solution are computed using FE-MUSCL schemes of different nominal orders of accuracy and the patched-grid interface treatments of the Section III.

Figure 6 shows the L_{inf} norm of the errors with respect to the exact solution , defined as: $L_{\text{inf}}(\epsilon) = sup(|w_{i,j} - w_{i,j}^{exact}|)$, for the numerical solutions computed by using FD schemes of 3^{rd} order (FD3) and 5^{th} order (FD5) accuracy with numerical fluxes given by Equation 7, in conjunction with the overlapping grid method. Results show that the formal overall order of accuracy of the inner scheme is recovered by using interpolations of the same order or higher. Here, we use interpolation polynomials of order $2p+2$ in order to get a symmetric interpolation stencil and reduce interpolation errors. Similar results are obtained when using the FV schemes (Eq. 11) and the 3rd and 5th-order k-exact schemes (not reported for brevity). Figure 7 shows the L_{inf} norm of the error when using the FD schemes along with the fictitious grid method. In this case, the overall accuracy is sticked to order 2. This is due to the introduction of a second-order error term via the patched grid treatment, which does not cancels with the error introduced by the inner point fluxes. This proves that the use of an inner point discretization that is coherent with

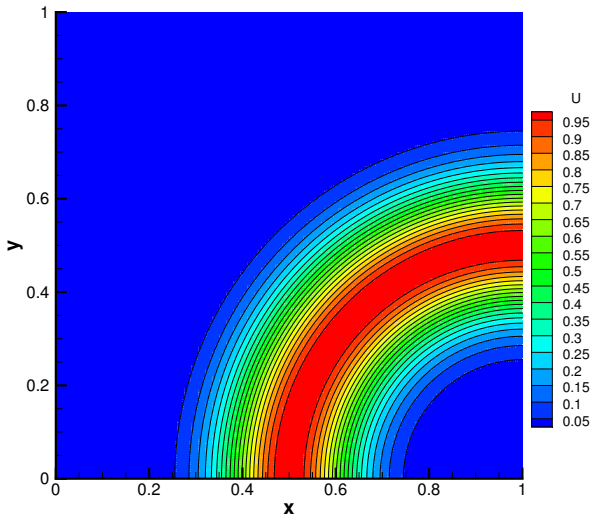

Figure 5. Exact solution for the circular advection problem.

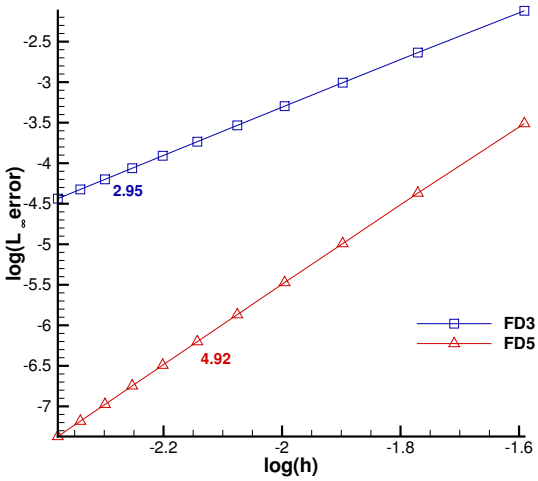

Figure 6. Circular advection problem. Accuracy of overlapping grid method.

the interface treatment is mandatory to recover overall high-order accuracy. Actually, if the fictitious grid method is used in conjunction with truly high-order FV schemes, the expected order of accuracy is recovered.

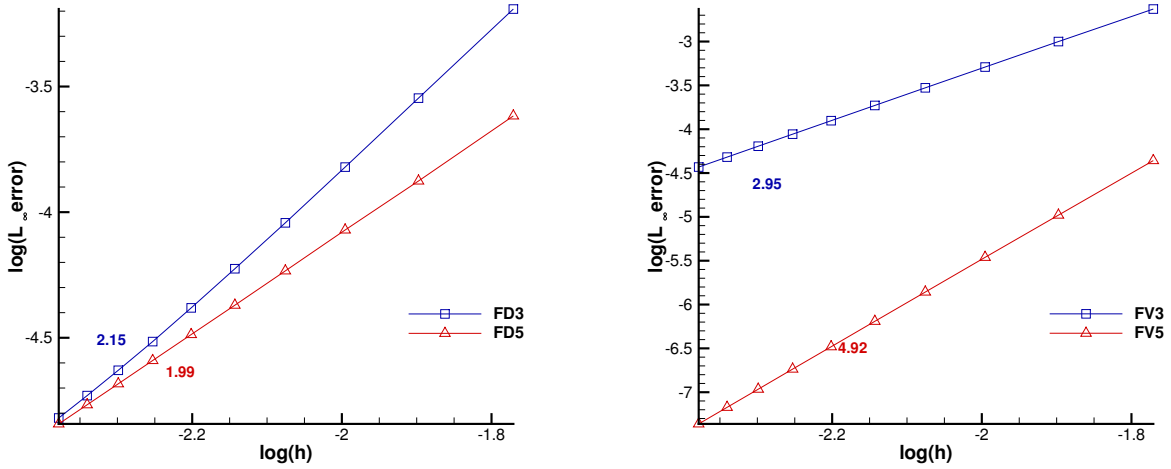

(a) FD (b) FV+integration

Figure 7. Accuracy of fictitious grid method - Conservative method

IV.B. Ringleb Flow

Next, the accuracy of the numerical method described above is investigated for a nonlinear set of equations and curvilinear meshes. For this purpose, we consider the so-called Ringleb flow,[20] for which an exact solution of the Euler equations is available. Solutions are computed by using two kinds of computational grids: single-block grids covering the whole computational domain and patched grids composed by two domains connected through a no-match interface (see Fig. 8). For each kind of grid, mesh resolution is progressively increased in order to check the behavior of the error with respect to the exact solution in terms of a characteristic grid size.

Single-block calculations are run using the nominally third-order accurate FD, FV and k-exact schemes. Then, calculations on patched grids are carried out by using both the overlapping grid and the fictitious grid methods described in Section III. An overall view of the solution (Mach number contours obtained by using the conservative interface treatment and a 3rd-rder k-exact scheme), as well as details of the patched grid, are provided on Fig. 8. The L_∞ norm of the error on the density field versus mesh size is represented in Fig. 9 for several schemes and interface treatments.

Figure 9(a) shows up the limitations of standard FV schemes when applied to non Cartesian grids: since the schemes do not take into account the actual grid geometry to construct the numerical fluxes, nominal accuracy is not preserved on curvilinear grids, and the actual convergence order is found to be equal to about 2 both for FD and FV schemes. On the contrary, when using a 3rd-order k-exact reconstruction of the solution over one cell, mesh deformations are automatically taken into account and the nominal convergence order is preserved even on general curvilinear grids.

Figure 9(b) shows the effect of the interaction between the inner-point scheme and the interface treatment on the overall convergence order for the fictitious grid method. Like in the preceding case, using FD schemes in conjunction with the fictitious grid method leads to an overall convergence order of about 2, which is lower than the order of convergence found for single-block computations, which in turn is already lower than the nominal one because of mesh deformations. On the contrary, when using the non conservative overlapping grid method or the fictitious grid method in conjunction with a truly high-order FV scheme, the nominal order of accuracy is preserved.

Finally, we investigate the impact of the interface treatment on mass conservation through the computational domain. Precisely, we compute and compare mass flow immediately upstream and downstream of the patched interface. The inner-point scheme in use is a 3rd-order k-exact scheme. For the overlapping grid method, the relative error on the computed mass flow across the interface is found to be equal to 10^{-4}, whereas for the fictitious grid method mass conservation is verified to machine accuracy (relative error of 10^{-15}).

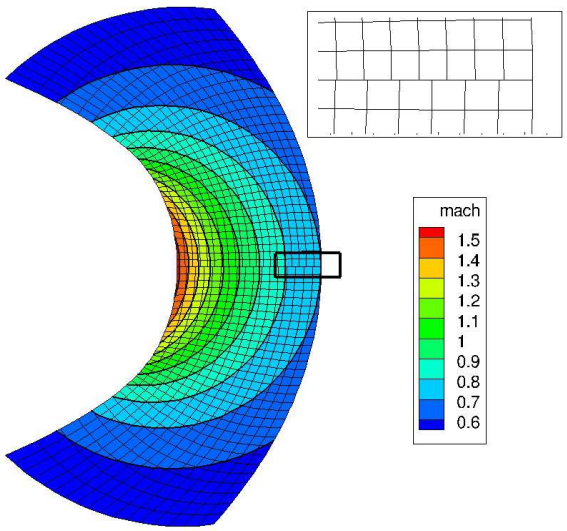

Figure 8. Ringleb flow case: no-match grid and overview of the Mach number contours (3rd-order k-exact scheme, conservative interface treatment.

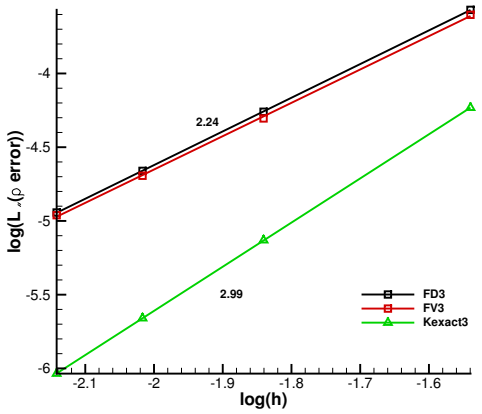

(a) Order of convergence for single-block computations

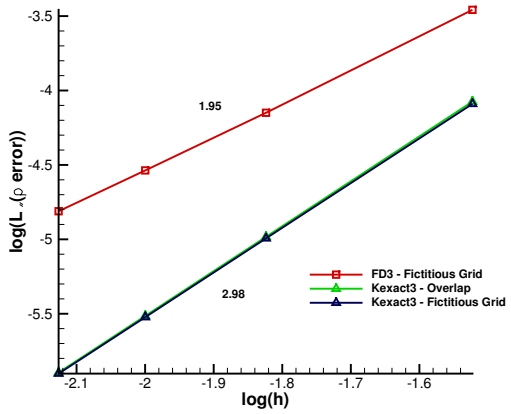

(b) Order of convergence for patched-grid computations

Figure 9. Ringleb flow. Numerical errors for several numerical schemes and interface treatments.

In the following, we retain only the third-order k-exact FV method along with the fictious grid interface treatment, which is expected to ensure high-order accuracy and conservation.

IV.C. Transonic flow through Delery nozzle C

To check the impact of interface treatments on the conservation properties of the numerical method, we consider the inviscid transonic flow through the so-called Delery nozzle C.[21] The flow is characterized by an inlet Mach number equal to 0.4, and a pressure ratio equal to 0.673, which leads to the formation of a shock wave in the divergent. The computational domain is discretized by a 2-block patched-grid. Subsonic inlet and outlet conditions based on flow characteristics are imposed at the leften and righten boundaries of the domain, respectively, whereas slip conditions are prescribed along the lower and upper boundaries. The interface between the 2 blocks is located slightly downstream of the bump (see Figure 10). The upstream block is composed by 94×64 cells and the downstream one by 54×65 cells.

Figure 10. Delery nozzle, Mach number contours.

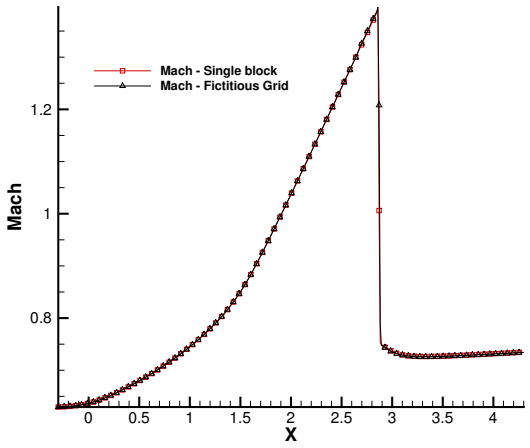

Figure 11. Middle slice $y = 0.5$

Figure 10 provides an overall view of the solution computed by using the third order k-exact FV scheme and the fictitious grid interface treatment. The shock is well captured and non oscillatory. The patched grid solution is superposed to the one obtained by using a single-block grid composed by 148×64 cells (See Figure 11).

To check if the conservation property is verified, we computed the conservation rate:

$$\delta Q[\%] = \frac{Mass\ flow\ out\ -\ Mass\ flow\ in}{Mass\ Flow\ out} \cdot 100 \tag{15}$$

Results are shown in Table 1: the non-conservative overlapping grid method leads to significant losses of mass flow rate, on the contrary the fictitious grid treatment gives a conservation rate close to the single-block computation.

Methods	$\delta Q[\%]$
k-exact - Single-block	$-2.7905 \cdot 10^{-5}$
k-exact - Overlap method - Two blocks	0.07656
k-exact - Fictitious grid - Two blocks	$-2.6812 \cdot 10^{-5}$

Table 1. Mass flow conservation errors for the transonic Delery bump C.

IV.D. LS89 VKI Turbine

The last test case is an inviscid transonic flow through a planar cascade of turbine stator blades. The test case is described in Ref.[22] The inlet flow angle is set equal to 0^0 and the pressure ratio across the turbine is $P_i/P_{i0} = 0.48$, which leads to transonic flow conditions and to the formation of a shock wave at the blade trailing edge. The computational grid contains approximately $10,576$ cells and is composed by five blocks (See Table 2),the stator is discretised by an O-shaped grid around the blades and four H-shaped blocks for inlet. The patched-grid interface is make by changing the number of cell in J direction of the last block. The shock crosses the patched-grid interface.

Block	Grid Size
O1	273×12
H1	25×49
H2	137×33
H3	10×65
H4-Match	24×65
H4-Patched-Grid	24×66

Table 2. Discretization of planar turbine cascade

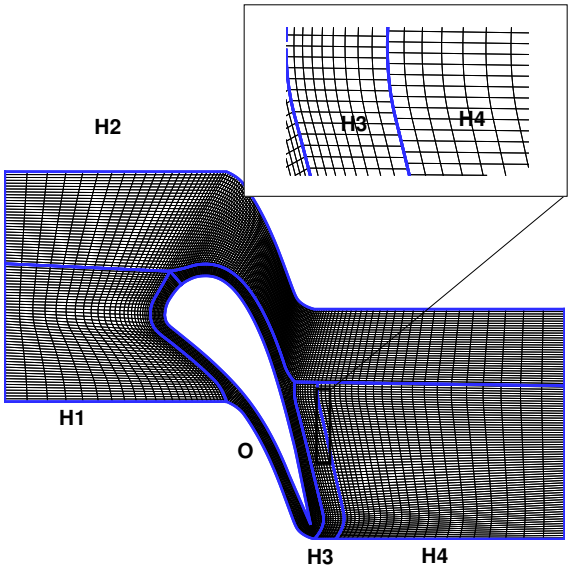

Figure 12. LS89 - No-match Mesh

Figure 13 provides overall views of the solutions obtained by using a matching and a patched interface be-

tween blocks $H3$ and $H4$. The solutions are practically identical, which provides a qualitative demonstration of the accuracy of the present patched-grid interface treatment.

To compare in more detail the two computations, a slice is made at $x = cst$. Figure 14 shows distributions of the Mach number along this slice for the matching and patched-grid interface. The two solutions are practically superposed, namely in terms of shock location and intensity, which validates the present methodology.

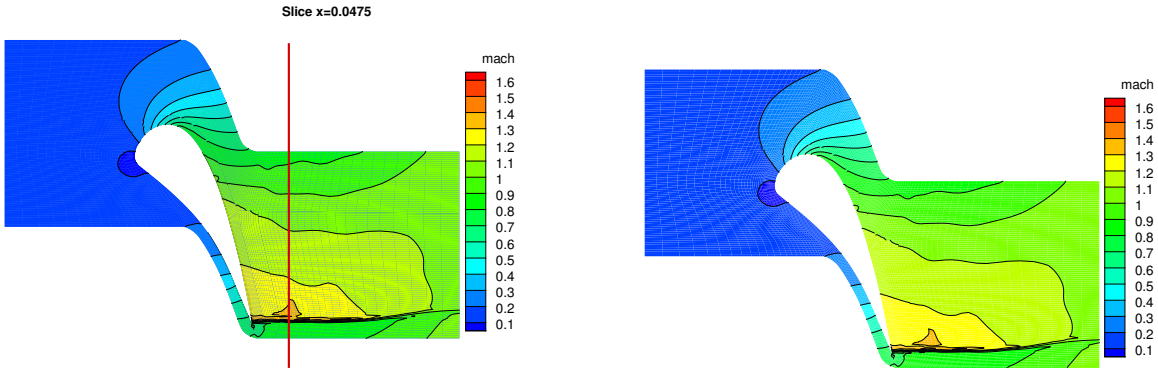

(a) LS89 - Mach number Patched-Grid

(b) LS89 - Mach Number Match

Figure 13. LS89 Turbine stage - Quantitative comparison between match and no-match computations

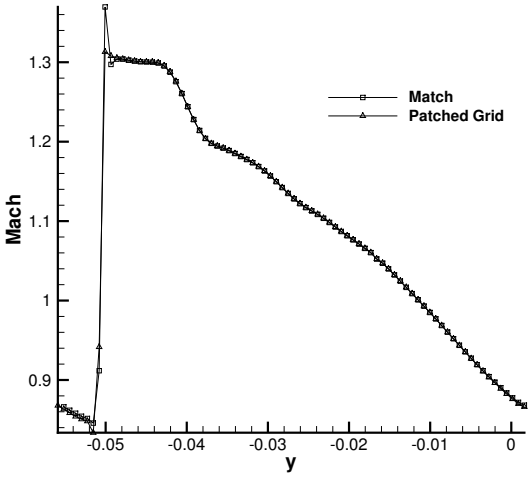

Figure 14. Mach number slice along $x = 0.0475$

V. Conclusion

A conservative and high-order patched-grid interface treatment is constructed and compared to a non conservative high-order patched-interface treatment. Numerical results for well-documented test cases show that the proposed methodology, based on the use of a fictitious grid around the interface, ensures mass conservation and proper shock capturing while achieving high overall accuracy. This represents a clear

improvement over the high-order overlapping method which ensures high-order accuracy but introduces significant errors on the mass flow rate, especially when the flow is highly compressible. This kind of error is not acceptable for turbomachinery constructors, which require that mass flow rate is conserved to machine accuracy. The proposed methodology allows to achieve the prescribed accuracy.

As a side effect, present calculations showed the importance of using a truly high-order FV scheme in conjunction with the fictitious grid method to preserve the nominal order of accuracy of the spatial discretization when using curvilinear and patched grids.

References

[1]Michel, B., Cinnella, P., and Lerat, A., "Multiblock residual-based compact schemes for the computation of complex turbomachinery flows," *International Journal of Engineering Systems Modelling and Simulation*, Vol. 3, No. 1, 2011, pp. 2–15.

[2]Rai, M. M., "An implicit, conservative, zonal-boundary scheme for Euler equation calculations," *Computers & fluids*, Vol. 14, No. 3, 1986, pp. 295–319.

[3]Mohan Rai, M., "A conservative treatment of zonal boundaries for Euler equation calculations," *Journal of Computational Physics*, Vol. 62, No. 2, 1986, pp. 472–503.

[4]Thomas, J. L., Walters, R. W., Reu, T., Ghaffari, F., Weston, R. P., and Luckring, J. M., "A patched-grid algorithm for complex configuration directed towards the F/A-18 aircraft," *Rep./AIAA*, Vol. 89, 1989, pp. 0121.

[5]Lerat, A. and Wu, Z., "Stable conservative multidomain treatments for implicit Euler solvers," *Journal of computational physics*, Vol. 123, No. 1, 1996, pp. 45–64.

[6]Tucker, P., "Computation of unsteady turbomachinery flows: Part 1Progress and challenges," *Progress in Aerospace Sciences*, Vol. 47, No. 7, 2011, pp. 522–545.

[7]Tucker, P., "Computation of unsteady turbomachinery flows: Part 2LES and hybrids," *Progress in Aerospace Sciences*, Vol. 47, No. 7, 2011, pp. 546–569.

[8]Rai, M. M., "A direct numerical simulation of transition and turbulence in a turbine stage," *AIAA*, Vol. 584, 2009, pp. 5–8.

[9]Rai, M. M., "Direct Numerical Simulations of Transitional and Turbulent Flow on a Turbine Airfoil," *Journal of Propulsion and Power*, Vol. 26, No. 3, 2010, pp. 587–600.

[10]Pärt-Enander, E. and Sjögreen, B., "Conservative and non-conservative interpolation between overlapping grids for finite volume solutions of hyperbolic problems," *Computers & fluids*, Vol. 23, No. 3, 1994, pp. 551–574.

[11]Berger, M. J., "On conservation at grid interfaces," *SIAM journal on numerical analysis*, Vol. 24, No. 5, 1987, pp. 967–984.

[12]Berger, M. J., "Stability of interfaces with mesh refinement," *Mathematics of computation*, Vol. 45, No. 172, 1985, pp. 301–318.

[13]Wu, Z.-N., "Steady and unsteady shock waves on overlapping grids," *SIAM Journal on Scientific Computing*, Vol. 20, No. 5, 1999, pp. 1851–1874.

[14]Lerat, A. and Corre, C., "Higher order residual-based compact schemes on structured grid," *Discretization Methods, Von Karman Institute*, 2006, pp. 1–105.

[15]Lerat, A. and Rezgui, A., "Schémas dissipatifs précis à l'ordre trois pour les systèmes hyperboliques," *Comptes rendus de l'Académie des sciences. Série II, Mécanique, physique, chimie, astronomie*, Vol. 323, No. 6, 1996, pp. 397–403.

[16]Rezgui, A., Cinnella, P., and Lerat, A., "Third-order accurate finite volume schemes for Euler computations on curvilinear meshes," *Computers & fluids*, Vol. 30, No. 7, 2001, pp. 875–901.

[17]Saunier, O., "Mesh adaptations with high order schemes for Euler equations." *PhD thesis, Arts et Metiers ParisTech*, 2008.

[18]Barth, T. J. and Frederickson, P. O., "Higher order solution of the Euler equations on unstructured grids using quadratic reconstruction," *AIAA paper*, Vol. 13, 1990, pp. 8–11.

[19]Haider, F., Brenner, P., Courbet, B., and Croisille, J.-P., "Efficient implementation of high order reconstruction in finite volume methods," *Finite Volumes for Complex Applications VI Problems & Perspectives*, Springer, 2011, pp. 553–560.

[20]Ringleb, F., "Exakte Lösungen der Differentialgleichungen einer adiabatischen Gasströmung," *ZAMM-Journal of Applied Mathematics and Mechanics/Zeitschrift für Angewandte Mathematik und Mechanik*, Vol. 20, No. 4, 1940, pp. 185–198.

[21]Délery, J., Marvin, J., and Reshotko, E., "Shock-wave boundary layer interactions," Tech. rep., DTIC Document, 1986.

[22]Arts, T., Lambertderouvroit, M., and Rutherford, A., "Aero-thermal investigation of a highly loaded transonic linear turbine guide vane cascade. A test case for inviscid and viscous flow computations," *NASA STI/Recon Technical Report N*, Vol. 91, 1990, pp. 23437.